

# Comparing central and upwind flux averaging schemes of overlapping finite volume method for simulation of spillway flow with shock waves

S.R. Sabbagh-Yazdi, N.E. Mastorakis, and S.M. Hosseini-Gelekolai

**Abstract**—This paper presents the comparison between the results of central and upwind flux averaging at the boundary edges of overlapping unstructured finite volumes for simulating super-critical free surface flow in channels with non-parallel side walls. The developed models compute water depth and velocity components using depth average continuity and motion equations which are mapped parallel to the bed surface for supercritical flows. This model evaluates two-dimensional velocity patterns and shockwaves. The governing equations are discretized utilizing overlapping cell vertex finite volume method on triangular unstructured meshes. The numerical oscillations of explicit solution procedure are damped out using either artificial viscosity scheme or upwind averaging fluxes at control volume boundary edges. The algorithm of evaluation of the fluxes at edges and artificial dissipation terms at nodes is adopted for unstructured meshes. Using both schemes, no additional dissipation is introduced to the computed flow and shockwaves are simulated accurately. The accuracy of results is assessed by simulating super-critical flow in two chute canal with expanded and contracted walls and using comparison between the computation results with the reported experimental measurements. Then, the model is applied for modeling a real world case of flow from dam reservoir to a chute spillway.

**Keywords**—Numerical Simulation, Upwind Flux, Finite Volume Method, Super-Critical Flow

## I. INTRODUCTION

In order to calculate flow parameters such as velocity, depth and Froude number, and to check cavitation phenomena, it is necessary to predict flow patterns in chutes. Furthermore, when the width of channel is expanded or contracted some steady shock waves are generated and propagate downstream in the hydraulic system. The position and direction of these waves remains constant for steady flows. The height and speed of the shock waves are important

parameters in design of side walls along channels and the self aeration flow characteristics.

Many researches were reported in this regard, using various numerical schemes such as the Method of Characteristics, Finite Difference Method (FDM), Finite Element Method (FEM), and the Finite Volume Method (FVM).

In this paper, the shallow water equations, which for supercritical flows are mapped parallel to the bed surface, are considered for mathematical modeling of two-dimensional flows. Numerical computations of two-dimensional super-critical flow using finite volume method is performed using two methods of central and upwind flux averaging at the overlapping unstructured finite volume boundary edges. The central scheme requires additional artificial viscosity terms for damping numerical oscillations of explicit solution while application of upwind averaging relaxes the requirement for additional artificial viscosity terms.

The numerical model utilized for present computations are originally developed by the first author and here after verification of its accuracy, it is applied to a real world spillway flow case in which subcritical flow in dam reservoir with arbitrary boundaries is combined with supercritical flow in a chute spillway with non-parallel walls, central pier and multi-slope bed.

## II. MATHEMATICAL MODEL

The mathematical model for spillway flow is considered as the set of shallow water equations. However, considering mild slope is the basic assumption for derivation of these equations. This assumption restricts application of these equations for flow problems with steep bed slope, particularly for the supercritical cases. Therefore, for supercritical flow the equations are modified for a coordinate system with two axes ( $x'$  and  $y$ ) parallel to the bed surface [1].

$$\frac{\partial h'}{\partial t} + \frac{\partial(h'u')}{\partial x'} + \frac{\partial(h'v')}{\partial y} = 0 \quad (1)$$

$$\begin{aligned} \frac{\partial(h'u')}{\partial t} + \frac{\partial(u'h'u')}{\partial x'} + \frac{\partial(vh'u')}{\partial y} + \frac{\partial}{\partial x'} \left[ h' \frac{gh'}{2 \cos \alpha} \right] \\ = gh' \sin \alpha - gh'S_{fx'} \end{aligned} \quad (2)$$

Manuscript received Sept. 20, 2007; Revised received February 1, 2008  
Saeed-Reza Sabbagh-Yazdi is Associate Professor Civil Engineering Department of K.N. Toosi University of Technology, 1346 Valiasr St. Tehran, IRAN (phone: +9821-88521-644; fax: +9821-8877-9476; e-mail: SYazdi@kntu.ac.ir).

Nikos E. Mastorakis, is Professor of Military Institutes of University Education (ASEI) Hellenic Naval Academy, Terma Chatzikyriakou 18539, Piraeus, GREECE

Seied-Mojtaba Hosseini-Gelekolai is BSc graduate of Civil Engineering Department of K.N. Toosi University of Technology, 1346 Valiasr St. Tehran, IRAN (hosseinigelekolai@gmail.com).

$$\frac{\partial(h'v)}{\partial t} + \frac{\partial(u'h'v)}{\partial x'} + \frac{\partial(vh'v)}{\partial y} + \frac{\partial}{\partial y} \left[ h' \frac{gh'}{2 \cos \alpha} \right] = -gh'S_{fy} \quad (3)$$

In which,

$$S_{fx'} = \frac{n^2 u' \sqrt{u'^2 + v^2}}{h'^{4/3}} \quad (4)$$

$$S_{fy} = \frac{n^2 v \sqrt{u'^2 + v^2}}{h'^{4/3}} \quad (5)$$

In these equations  $x'$  is the axis tangential to the chute slope (which is horizontal for subcritical cases) and  $y$  is the same as the  $y$  axis in the global coordinate system;  $u'$  and  $v$  are the velocity components in  $x'$  and  $y$  directions, respectively.  $h'$  is the flow depth perpendicular to the chute bed surface and  $g$  is gravity acceleration;  $\alpha$  is the chute angle (which is zero for subcritical flow);  $S_{fx'}$  and  $S_{fy}$  are the bed surface friction slopes in  $x'$  and  $y$  directions, respectively and  $n$  is Manning's friction coefficient [2].

### III. NUMERICAL SOLUTION MODEL

In this paper, in order to discretize the sloping depth average equations, the overlapping cell vertex finite volumes which are formed by some triangles meeting at each nodal point (Fig. 1) are applied. The two-dimensional governing equations in the conservative form can be written as:

$$\frac{\partial Q}{\partial t} + \frac{\partial F_x}{\partial x} + \frac{\partial F_y}{\partial y} = \frac{\partial G_x}{\partial x} + \frac{\partial G_y}{\partial y} + S \quad (6)$$

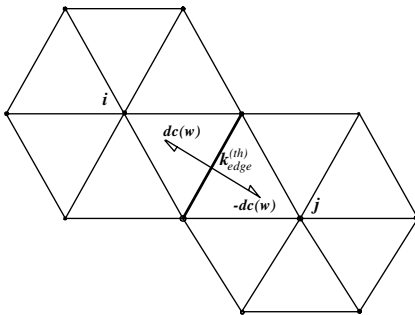


Fig.1, Two overlapping control volumes

Integrating over each control volume  $\Omega$  using the Finite Volume Method, the discrete form of equations takes the general form of :

$$Q^{n+1} = Q^n - \frac{\Delta t}{\Omega} \sum_m [(F_x \Delta x - F_y \Delta y) + (G_x \Delta x - G_y \Delta y)]_m - S_i \Delta t \quad (7)$$

Here,  $\bar{F}_x$  and  $\bar{F}_y$  are the convective fluxes while  $\bar{G}_x$  and  $\bar{G}_y$  are hydrostatic pressure fluxes. The value of dependent variables  $Q$  at nodes can be used for computation of average fluxes at control volume boundary edges as:

$$F_x = F_x(Q), F_y = F_y(Q) \quad (8)$$

The above mention fluxes are usually computed by averaging of fluxes at associated nodes of control volume boundary edges. Two averaging methods are described in following sections. The first method which uses two end nodes of boundary edges of the control volumes for flux averaging procedure is identical to central schemes (for regular meshes) while the second method which uses the aforementioned node plus an upstream node is an upwind scheme.

### IV. THE CENTRAL FLUX AVERAGING

It can be shown that if two end nodes of control volume boundary edges are used for computation of average fluxes of using following relation the resulted formulation approaches the central differencing scheme for meshes with relatively regular cell sizes.

$$\bar{F} = (F_1 + F_2) / 2 \quad (9)$$

Therefore, application of this averaging method may give rise to numerical oscillation and would destroy the stability and accuracy of explicit computation procedure. To stabilize the explicit solution of hyperbolic equations adding artificial viscosity to the numerical formulation is one of the efficient techniques. The Laplacian operator ( $\nabla^2 Q$ ) with depth switch  $S_h$  provides a suitable mechanism for damping superior numerical oscillation near shock waves.

$$\nabla^2 Q = S_h \varepsilon_2 \lambda_{ij} \sum_{j=1}^{Ne} (Q_j - Q_i) \quad (10)$$

However, for the regions with smooth variations of flow variables application of Biharmonic operator ( $\nabla^4 Q$ ) may be beneficial.

$$\nabla^4 Q = \varepsilon_4 \lambda_{ij} \sum_{j=1}^{Ne} (\nabla^2 Q_j - \nabla^2 Q_i) \quad (11)$$

$\lambda_{ij}$  is a scaling factor and is computed using the maximum value of the spectral radii of every node  $i$ . The coefficient of the artificial dissipation term  $\varepsilon_2$  and  $\varepsilon_4$  should be tuned to minimum value required for stabilizing the solution procedure.

#### V. THE UPWIND FLUX AVERAGING

In previous section the value of fluxes is calculate at the center of each boundary edge of control volumes. Here in order to make upwind characteristics, three point of cells attached to the boundary edges of control volume are utilized to compute the fluxes required for finite volume calculations.

The value of dependent variables at three nodes (including two nodes at both ends the desired edge and upstream node.) can be used for computation of average fluxes at boundary edges as:

$$\bar{F} = \theta F_{up} + \frac{1-\theta}{2}(F_1 + F_2) \quad (12)$$

Where, the weighting coefficient  $\theta$  can be chosen between 0. to 0.333. On regular meshes, above mentioned formulation with  $\theta = 0$  may produce numerical results similar to second order central differencing scheme. However, if one uses  $0.33 < \theta$ , the scheme will produce numerical results similar to the first order schemes. Using the values of  $0 < \theta < 0.33$  would result a simple oscillation free upwind scheme (with the accuracy somehow between first and second order) and hence, there would be no need to add any extra numerical dissipation to the computed residuals.

The upstream node may be considered proportional to the direction of computed value of normal velocity  $\bar{U}_k$  at the edge by using following formulations. The up and down nodes can be distinguished using the sign of the dot product of unit normal and velocity vector of the edge ( $\bar{U}_k \cdot \hat{n}$ , where  $\hat{n} = (\Delta y \hat{i} - \Delta x \hat{j}) / \Delta s$  is unit normal vector of the edge).

In order to compute upstream convective flux,  $F_{UP}$ , the dependent variable  $Q_{UP} = Q(Up Node)$  may be used. The upstream node may be considered proportional to the direction of computed value of normal velocity  $\bar{V}_e = \bar{u}_i + \bar{v}_j$  at the edge by using following formulations. The up and down nodes can be distinguished using the sign of the dot product of  $V_n = \bar{V}_e \cdot \hat{n}$ , where  $\hat{n} = (\Delta y \hat{i} - \Delta x \hat{j}) / \Delta s$  unit normal vector of the edge (Fig. 2).

Using this simple upwind scheme will produce oscillation free results, and hence, there would be no need to add any extra numerical dissipation to the computed residuals.

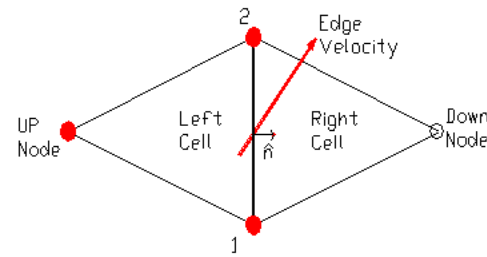


Fig.2, Two adjacent triangular cells

#### VI. ASSESSMENTS OF THE MODELS

First, the quality of the result of two schemes of central and upwind averaging in the model are assessed by comparison between the numerically simulated flow parameters of oblique hydraulic jump in a canal with a contraction in the left side wall of the canal for which reported results are available [3].

Then, in order to evaluate the computational results of two central and upwind schemes to simulate free surface flow in channel; data of the results of the model are compared with a experimental test measurements of the previous workers on super-critical flow in two canals with contracting [4] and expanding width [5]. In these canals, flow regimes are super-critical, thus two parameters of flow (depth and velocity) are imposed at the upstream of the canals.

In following super-critical flow cases, depth and velocity of the flow in upstream are imposed at upstream flow boundary. Therefore, the flow parameters are computed at downstream of the channel by numerical model.

##### A. Oblique Jump

In this section, comparisons are made between the results of two numerical schemes for an oblique hydraulic jump for which the details of the test case are considered similar to the case utilized by previous researchers are presented [3].

The canal with certain aspect ratio ( $B/h1 > 6$ ,  $L/h1 > 11.8$  where  $h1=0.1$ ) is used to generate unstructured triangular mesh. The canal is contracted by diverting the left side wall of the canal by a constant angle of 12 degree (Figure 3). The method Delaunay triangulation is used to generate the unstructured mesh. This method provides the ability of local refinement of the mesh by considering points and line sources [6]. Since the angle of the hydraulic jump from the analytical solution is known ( $\beta=25.505$  degree), the mesh is fined along a line with similar angle. The finalized unstructured mesh for present numerical simulation contains 1376 nodes, 2585 cells and 3960 edges (Fig. 3).

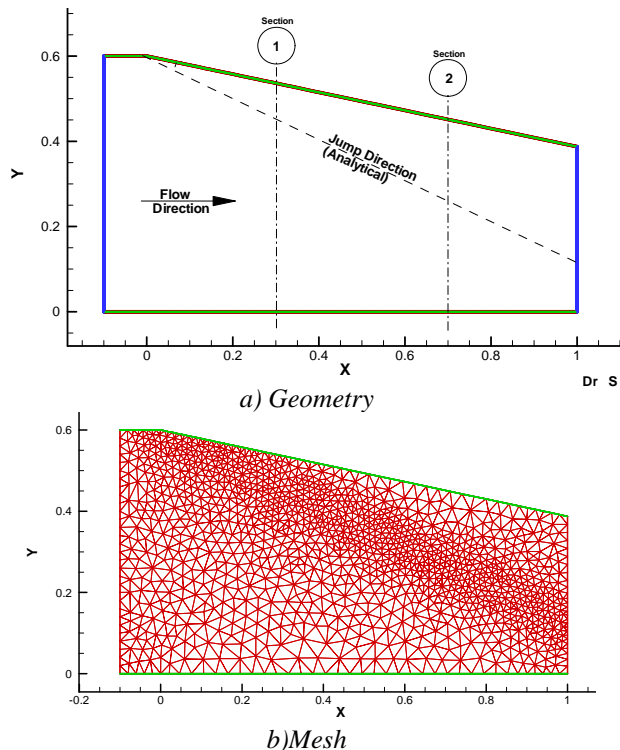


Fig.3, Geometry of the canal and Unstructured triangular mesh for the oblique jump (dimensions in meter)

The upstream Froude number is considered as 4. Therefore, the upstream flow depth and velocity are considered as  $0.1m$  and  $3.982m/s$ . Figure 4 present the convergence behavior of two flux averaging schemes.

Figure 5 demonstrates computed depths from central and upwind flux averaging schemes. For the computation of this case (using both schemes) on a Pentium IV (2.4 MHz) Personal Computer the  $CFL=3$  are used and CPU time consumption were measured as 7.14 and 6.82 seconds for central and upwind flux averaging schemes, respectively. It worth noting that according to the analytical solution for  $\beta = 25.505$  degree the depth and velocity after jump can be calculated using the ratios of  $h_2/h_1=1.987$  and  $v_2/v_1 = 0.9282$ , respectively.

In figure 6, the comparison between the reported analytical depth and numerically simulated water surface (using central and upwind flux averaging) along some cross sections of the canal are plotted. As can be seen, the upwind flux averaging scheme presents milder slope than the central flux averaging scheme for shock front but without any numerical oscillations close to the top and bottom of shock wave. Therefore, it can be stated that the results of the central flux averaging scheme are second order accurate in space, while the spatial accuracy of the upwind flux averaging scheme is somehow between the first and second order.

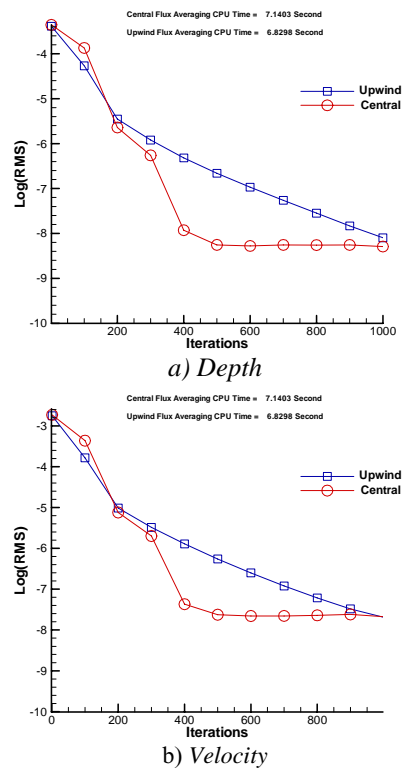


Fig.4, Convergence history of depth and velocity values for two flux averaging schemes (Oblique Jump)

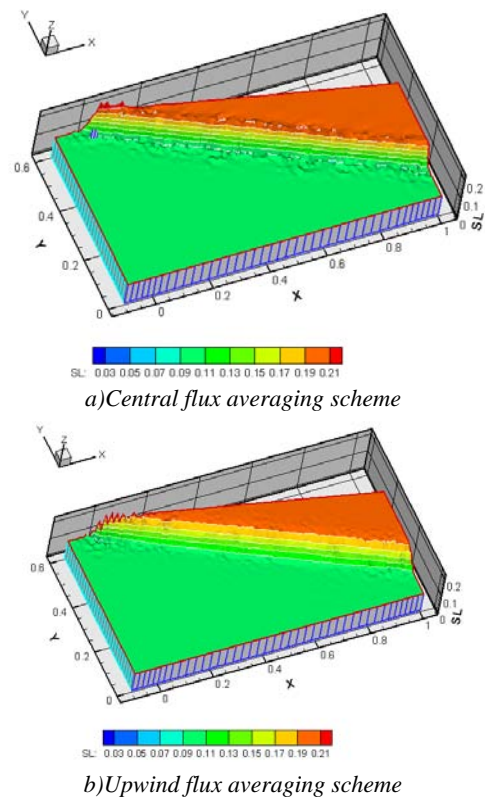


Fig.5, Computed water surface contours in oblique jump canal

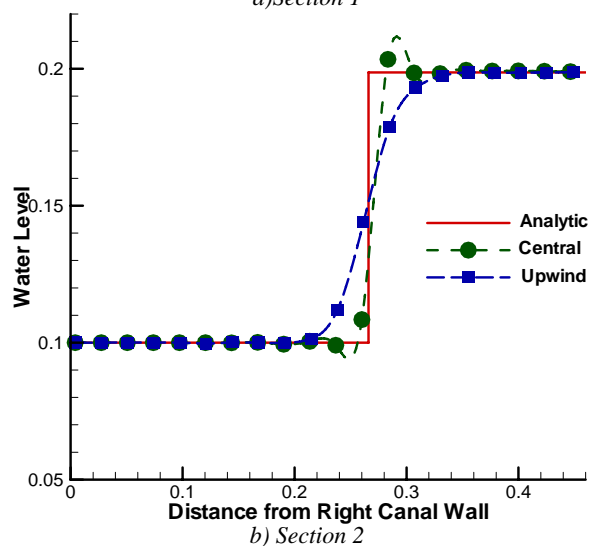
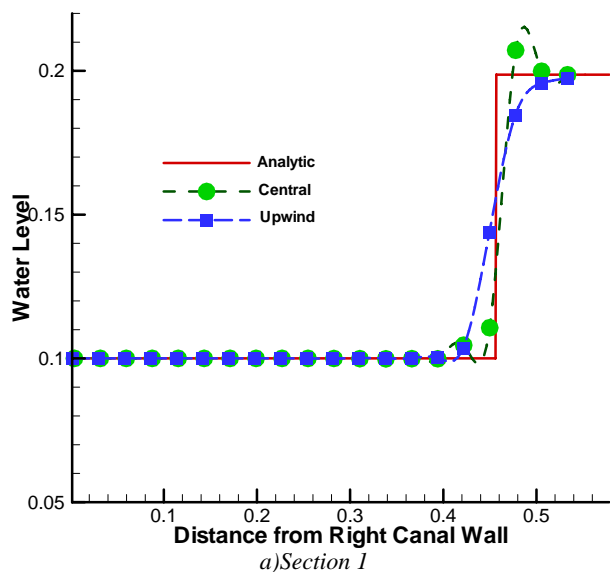


Fig.6, Comparison of computed water surface with the analytical solution in two sections

### B. Contracted canal without friction

In this part, the quality of the result of two schemes of central and upwind averaging in the model are assessed by simulation of flow in a contracted canal. The dimension of the canal is present at figure 7. The upstream flow depth and velocity are considered as 0.05m and 2.8m/s in the experimental set up report [4]. The utilized unstructured mesh for present numerical simulation contains 2340 nodes, 4417 cells and 6756 edges (Fig. 7).

Figure 8 present the convergence behavior of two different schemes of flux averaging. Figure 9 demonstrates computed depths from central and upwind flux averaging schemes. Figure 10 presents the comparison between the reported measured depth and numerically simulated water surface along the central are at the canal using central and upwind flux averaging.

For the computation of this case (using both schemes) on a Pentium IV (2.4 MHz) Personal Computer the CFL=3 are

used and CPU time consumption were measured 23.08 and 22.26 seconds for central and upwind schemes, respectively.

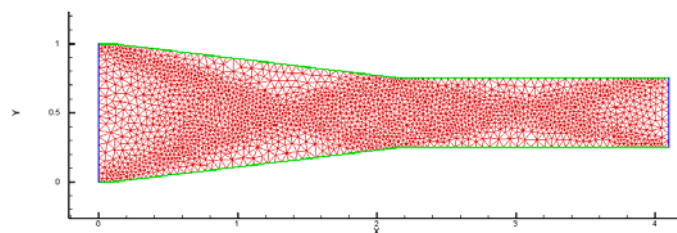


Fig.7, Unstructured triangular mesh for contracted canal (dimensions in meter)

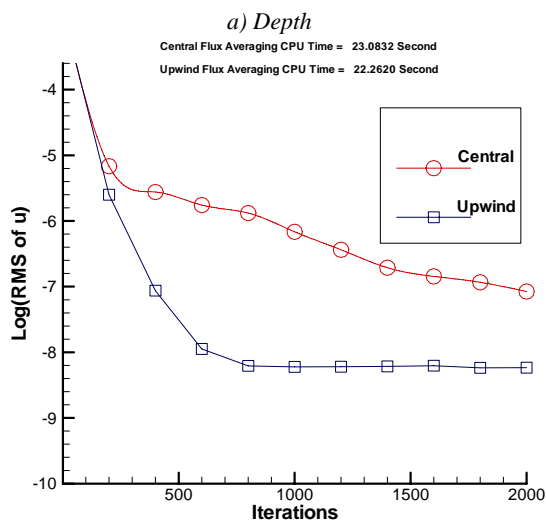
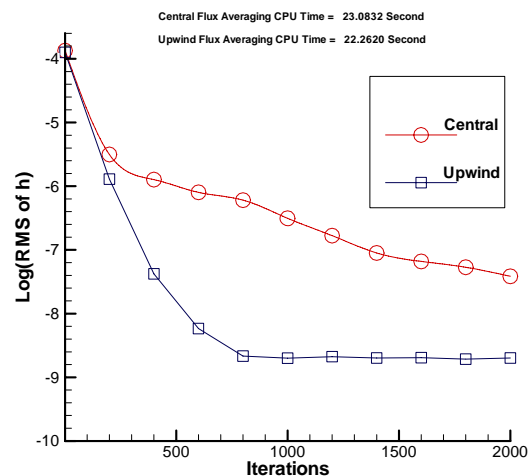
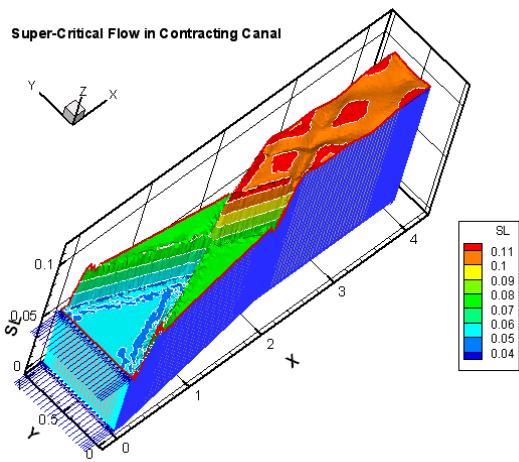
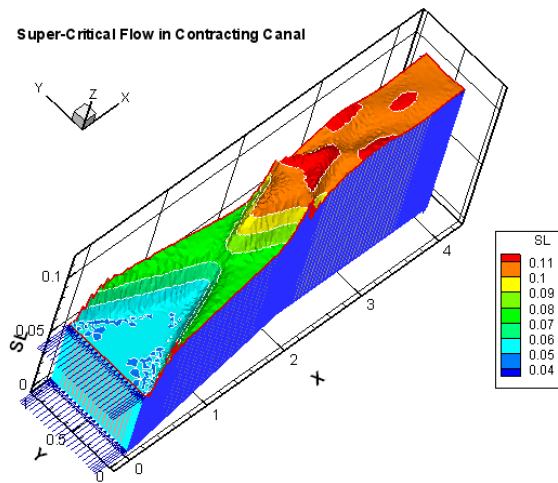


Fig.8, Convergence history of depth and velocity values for two flux averaging schemes (contracted canal)



a) Central flux averaging scheme



b) Upwind flux averaging scheme

fig.9, Computed water surface contours in contracted canal for upwind flux averaging scheme

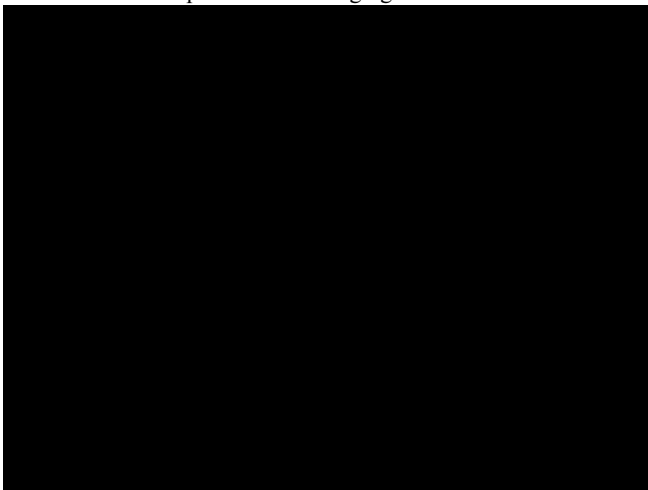


Fig.10, Water surface plots along center of contracted canal

### C. expanding canal with friction

In order to verify the accuracy of the super-critical flow simulation in a canal with expanded walls a canal that its geometry is presented in figure 11 is chosen. The bed surface

Chezy coefficient is reported as 70 and the inflow velocity and the upstream depth are measured as 1.4 m/s and 0.049 m. respectively according to the previous experimental work on the similar canal [5].

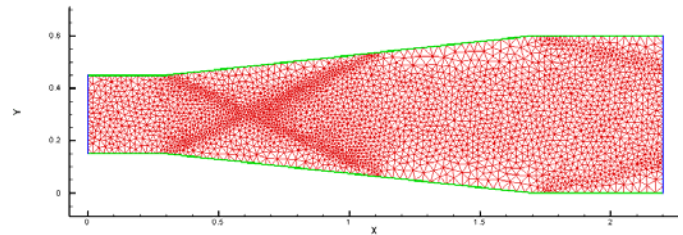
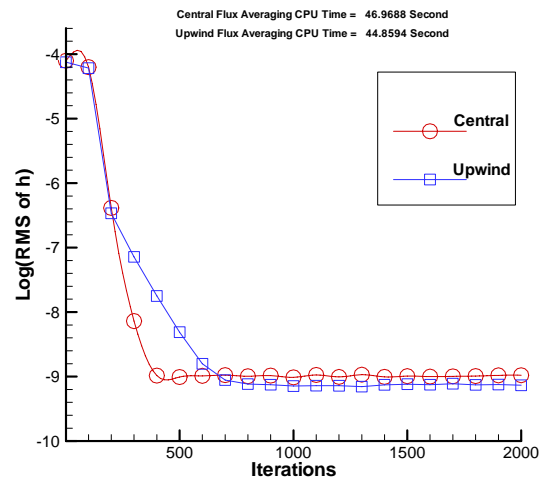
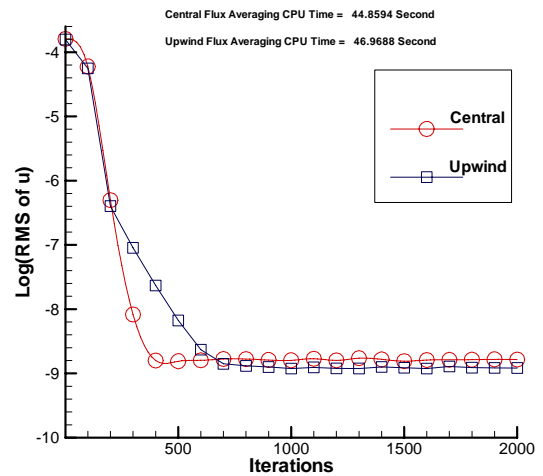


Fig.11, Unstructured triangular mesh for expanded canal (dimension in meter)



a)Depth

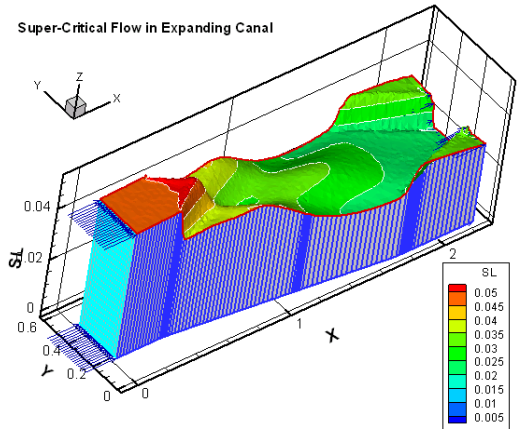


b)Velocity

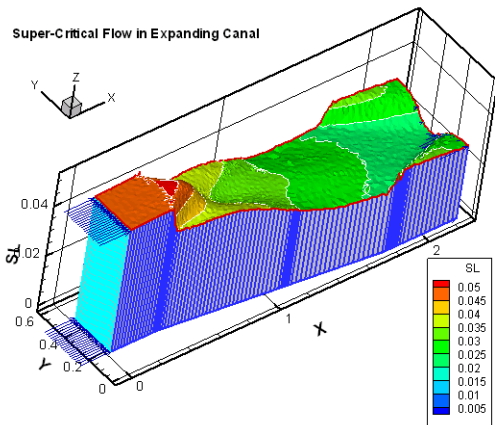
Fig.12, Convergence history of depth and velocity values for two schemes of flux averaging (expanded canal)

For numerical simulation of this case an unstructured mesh containing 3071 nodes, 8952 edges and 5882 cells is utilized ( Fig. 11 ). Figure 12 shows the convergence history flow depths for central and upwind flux averaging schemes. Figure 13, present some sample results of two abovementioned

schemes of the finite volume model. In figure 14, the results of computed water surfaces along the center of the canal resulted from both schemes are plotted and compared with the experimental data.



a) Central flux averaging scheme



b) Upwind flux averaging scheme

Fig.13, Computed water surface contours in expanded canal

It worth nothing that, the computation of the case (using both schemes) were performed by considering CFL=3 and CPU time consumption were measured 46.87 and 44.87 seconds on a Pentium IV (2.4 MHz) Personal Computer, for central and upwind schemes, respectively.

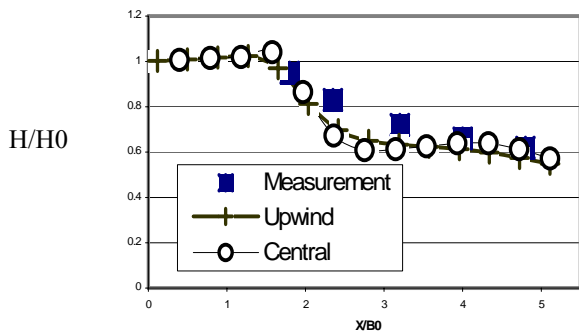


Fig.14, Computed depths and experimental measurements along center of expanded canal

## VII. APPLICATION OF THE MODEL

### A. model properties

In order to present the application of the model the spillway system of NAZLOCHAI in northwest of Iran has studied. The two parts of this chute spillway have different slopes. The plan view and longitudinal profile of the chute are shown in the following figures [7].

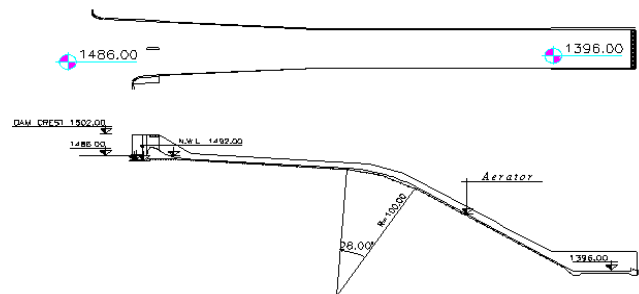


Fig.15, The plan and longitudinal profile of spillway

The geometry of this spillway is simulated from the approach channel up to the end of the chute. The geometrical model is converted to discrete form using triangular unstructured meshes with 7071 nodes and 13379 elements. Figure 16, shows 3-dimensional view of the region close to the reservoir, approach channel, odgee and beginning of the chute channel.

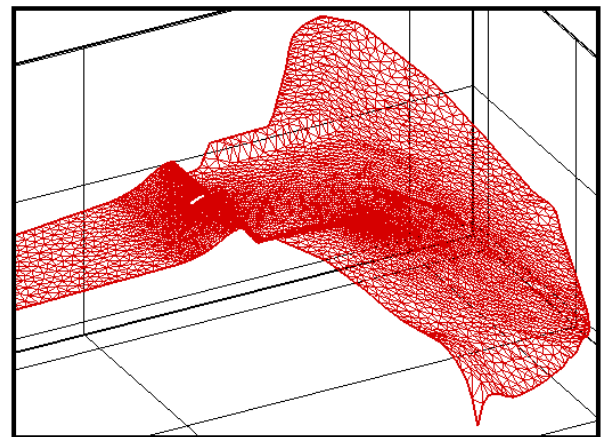
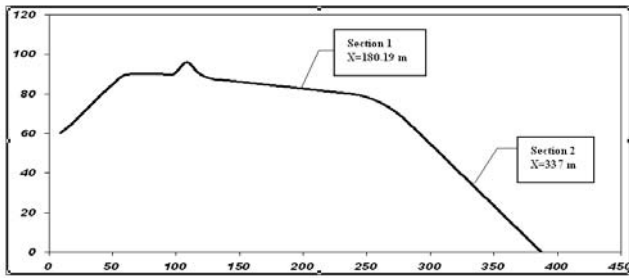


Fig.16, 3-dimensional meshed region

For numerical simulation, reservoir and approach channel are defined as subcritical regions, while, odgee and chute channel as supercritical regions. The stations in which numerical results are compared with the theoretical solution (using inviscid flow assumption) and experimental measurements are shown in a vertical section plotted in the following figure.



**Figure 1**

Fig.17, Specified sections for comparison of results

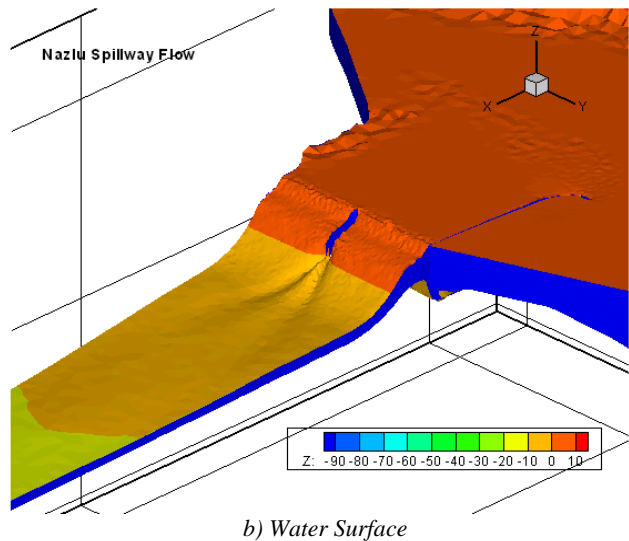
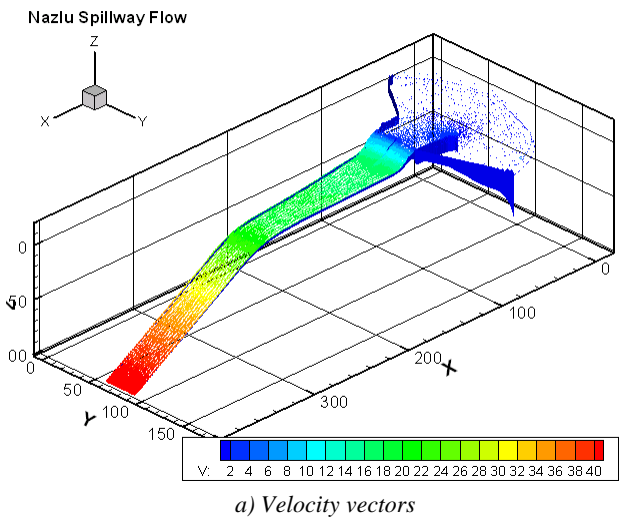


Fig.18, Results of numerical simulation in the form of color coded velocity vectors and water surface map

Samples of result of numerical simulation using central flux averaging scheme are shown in the form of color coded velocity vectors and water surface map in the above figures. As can be seen the model simulated the expected incline standing waves downstream of the central pier of the spillway. The mean velocity and depth of flow along the chute are

compared with theoretical inviscid solution and experimental measurements. Theoretical method uses equation ( $V = \sqrt{2gH}$ ) (without dissipation) in which  $V$  is mean velocity,  $H$  is height and  $g$  is gravity acceleration and for calculation of flow depth the theoretical method uses equation ( $d = q/V$ ) in which  $q$  is the discharge per unit width. The computed results for flow depth and mean velocity are compared with theoretical solution and experimental data in figures 19a and 19b, respectively.

The numerical results and theoretical solutions of the flow velocities at two specified stations are compared with the experimental measurements in the following table (1)

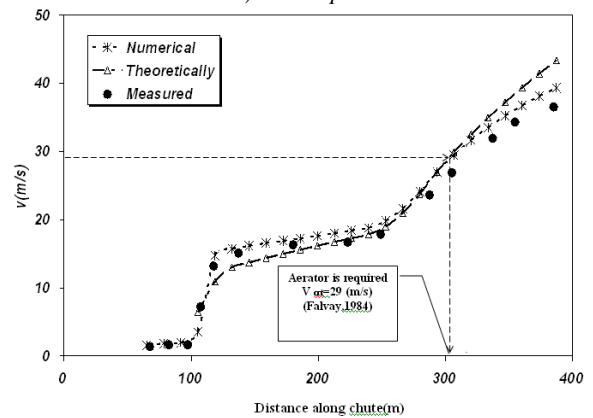
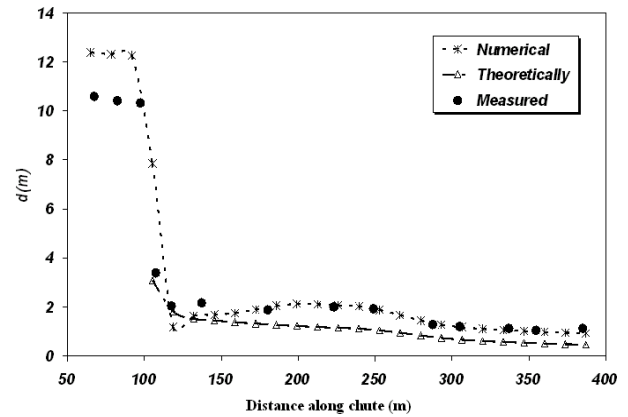


Fig.19, Comparison of results of numerical simulation with experimental data and theoretical solution

Table (1). Comparison of mean velocity errors

Discharge (m <sup>3</sup> /s)	Section	Experimental	Theoretical		Numerical	
			Quantity (m/s)	Error %	Quantity (m/s)	Error %
830	1	16.33	15.37	6	16.7	2.3
	2	31.94	35.61	11.5	34.01	6.5

The flow depth in approach channel presents considerable difference with experimental results. This difference is because of the fact that the model at this region computes just horizontal velocity components by assumption of negligible

vertical component. While, the flow in reality is fully three dimensional in the vicinity of the spillway crest upstream slope. Similar error may occur in experimental velocity measurements by horizontal Pitot tubes. The accumulation of these errors increases the differences between computed and measured values.

The computed results can be used to assess the potential of the cavitation along the chute. The results show that when velocity in chute spillways exceeds than 29 m/s, cavitation may occurred [8]. As shown in figure 19b velocities reach 29 m/s at  $x=305$  m. So design of aerator at the chute bottom is required to reduce risk of cavitation damage.

### VIII. CONCLUSION

Depth averaged equations of continuity and motions, which for supercritical flows are mapped parallel to the bed surface, are used as mathematical model for numerical simulation of two-dimensional super-critical free-surface flow in channels with non-parallel walls. The overlapping cell vertex finite volumes formed by gathering triangles connected to each computational node are used to convert the mathematical model into the discrete form, the governing equations. In this paper, the effects of non-parallel (contracted and expanded) walls are numerically investigated and shock waves similar to experimental observations are computed. The numerical oscillations due to explicit procedure of computations are damped out by application of two methods of central and upwind flux averaging at unstructured control volume boundaries.

For two-dimensional flow problems the numerical model successfully simulated the super-critical flow in contracted or expanded canals and the comparison with reported experimental works presents accepted agreement. The central averaging scheme needs adding the artificial dissipation terms while the upwind averaging provides relatively accurate results via robust and stable solution procedure without any additional artificial viscosity formulation. However, the upwind flux averaging scheme may need additional artificial dissipation with the constant coefficient considerably smaller than the central flux averaging scheme.

The developed model with central flux averaging scheme is examined for a real word problem of flow from dam reservoir to the chute spillway in which both subcritical and super critical flows should be solved simultaneously on a single mesh. The computed results present good agreements with experimental measurements in a combined subcritical flow in dam reservoir (with arbitrary boundaries) and supercritical flow in a chute spillway (with non-parallel walls, central pier and multi-slope bed). The model results show its ability of the model to capture standing incline shock waves in supercritical flows.

The developed model presented powerful and accurate performance for serving as a suitable tool to predict flow depth and velocity from dam reservoir over steep slopes chutes. In addition, this computational model can be used for

prediction of cavitation potentials along the chute spillways.

### IX. ACKNOWLEDGMENT

The technical support of this research work is provided by Water Research Institute (Iranian Ministry of Energy) in the form of providing experimental measurements.

### REFERENCES

- [1] S.R. Sabbagh-Yazdi, *Spillway Flow Modeling by Finite Volume Solution of Slopping Depth Averaged Equations on Triangular Mesh; Application to KAROUN-4*, 10th WSEAS International Conference on Applied Mathematics, Dallas (Texas), USA, 2006.
- [2] S.R. Sabbagh-Yazdi, E.N. Mastorakis & M.Zounemat-Kermani, *Velocity Profile over Spillway by Finite Volume Solution of Slopping Depth Averaged Flow*, WSEAS Transaction on Applied and Theoretical Mechanics, Issue 3, Vol.2, pp. 85-94, 2007.
- [3] O.F. Jimenez & M. H. Chaudhry, *Computation of Supercritical Free-Surface Flows*, Journal of Hydraulic Engineering, Vol. 114, No.4, pp. 377-395, 1988.
- [4] S.M. Kruger, Burgisser & P. Rutschmann., *Advances in Calculating Supercritical Flows in Spillway Contractions*, Hydro-informatics 98, Bavic & Larsen Balkema ,Rotterdam ,ISBN 90 5410 983 1, 1998.
- [5] M. Younus & M. H. Chaudhry, *A Depth-Averaged  $k-\epsilon$  Model for the Computation of Free Surface Flow*, Journal of Hydraulic Research, Vol.32, No.3, pp. 415-444, 1994
- [6] N.P. Weatherill, M.J. Marchant, O. Hassan & D. Marcum, *Grid Adaptation Using a Distribution at Sources Applied to Inviscid Compressible Flow Simulation*, Int. J. for Num. Meth. in Fluids, 19, pp. 739-794, 1994.
- [7] Final Report of Physical Hydraulic Model of NAZLOCHAI Spillway, Water Research Institute, Ministry of Energy, Iran, 2007.
- [8] H.T. Falvey, *Air-Water Flow in Hydraulic Structures*, USBR Engineering Monograph No. 41, Denver, Colorado·USA, 1980.

First Author's biography may be found in following site:  
<http://sahand.kntu.ac.ir/~syazdi/>